

Precise Assembly and Supramolecular Catalysis of Tetragonal- and Trigonal-Elongated Octahedral Coordination Containers

Tian-Pu Sheng¹², Can He¹, Zhenqiang Wang³, Guo-Zong Zheng¹, Feng-Rong Dai^{1*} & Zhong-Ning Chen^{1*}

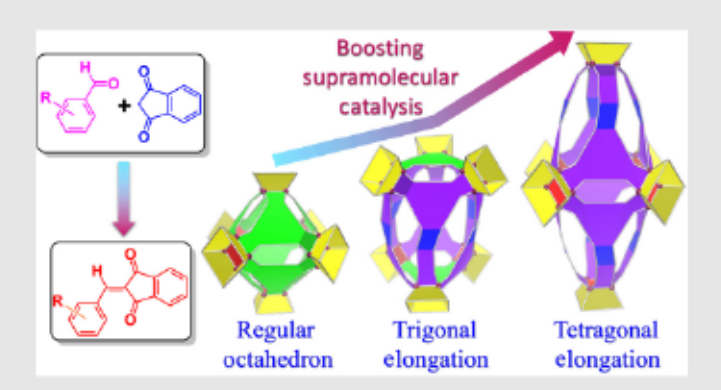
¹State Key Laboratory of Structural Chemistry, Fujian Institute of Research on the Structure of Matter, Chinese Academy of Sciences, Fuzhou, Fujian 350002, ²University of Chinese Academy of Sciences, Beijing 100049, ³Churchill-Haines Laboratories, Department of Chemistry, Center for Fluorinated Functional Materials, University of South Dakota, Vermillion, SD 57069-2390

*Corresponding authors: dfr@fjirsm.ac.cn; czn@fjirsm.ac.cn

Cite this: CCS Chem. 2021, 3, 1306-1315

The construction of distorted or irregular coordination polyhedrons with specific shapes and functionalities is highly challenging. Here, we demonstrate a viable strategy for attaining a severely distorted octahedral coordination container through precise geometrical manipulation of its nanocavity along the C3 or C4 axis to turn on its supramolecular catalysis. We constructed a tetragonal-elongated octahedral coordination container utilizing sulfonylcalix[4]arene-capped Co4 units as six vertexes and tetragonalelongated from single-arm lengthened 5-[(4-carboxybenzyl)amino]isophthalate (L) as eight triangular faces. Through the concomitant introduction of C3 -symmetry cyclohexane-1,3,5-tricarboxylate as a secondary linker to construct two equilateral triangular base surfaces and L to build six isosceles triangular side planes, trigonal antiprismatic architecture (trigonal-elongated octahedron) was attained. The elongated octahedral containers exhibited distinctly higher binding capacity and stronger binding affinity toward reaction substrates than that of regular octahedral

containers; thus, promoting geometry-dependent catalytic reactivity. Our geometrical manipulation strategy provides a viable approach for the convenient design of metal-organic materials with specific functionalities.



Keywords: coordination containers, host-guest interaction, supramolecular catalysis, acid-base dual catalysis, Knoevenagel condensation, elongated coordination octahedron

Introduction

Coordination containers, hollow supramolecular assemblies sustained by metal nodes and organic linkers, represent one of the most exciting classes of synthetic receptors. These host molecules have attracted a great deal of attention in the supramolecular chemistry community in recent years due to their well-defined

DOI: 10.31635/ccschem.021.202100987



polyhedral architectures and chemically tunable nanocavities, representing various promising applications in molecular recognition, 11-17 catalysis, 18-23 and so forth. Varying the symmetry and length of organic linkers is a key factor to achieve the geometric and size modulation of well-defined nanocavity in coordination containers, thereby providing an accessible approach to regulating host-guest chemistry properties to achieve the desired applications such as selective guest recognition and catalytic reactivity.²⁴⁻²⁷

While C_3 -symmetry tripodal ligands are well-known organic linkers for the construction of tetrahedral and octahedral coordination containers, 28-32 the utilization of tritopic ligands with a lower symmetry for the design of coordination containers is much less common, 33,34 presumably due to the stringent geometrical requirements for the assembly of high-symmetry polyhedral structures, even in rarer cases of severely distorted or irregular coordination polyhedral, constructed from mixed linkers of distinct sizes and shapes. Furthermore, symmetric tripodal organic linkers often occupy the faces of tetrahedral or octahedral coordination containers, likely to prevent specific guest molecules from accessing the endo cavity (where the host-guest chemistry is typically most active) and limit molecular recognition capability. Thus, judicious choice and elaborate design of various low-symmetry tripodal ligands are absolutely crucial for constructing distorted or irregular coordination polyhedrons with specific shapes, sizes, and functionalities.

As depicted in Scheme 1a, an octahedron could, in principle, be stretched along its C_4 axis through two opposite vertices or distorted along its C3 axis through the centroids of opposing triangular faces, generating a uniaxially elongated "octahedron" and trigonal antiprism, respectively. We envisioned that these two desymmetrization operations are more likely accessible than other possible geometrical manipulations since they are readily viable chemically. For example, the C4-elongated octahedral coordination container could be readily attained when eight single-arm lengthened tripodal linkers are bound to six metal-based units situated at octahedral vertexes. Obtaining the trigonal antiprism topology through significant elongation of octahedral architecture along the C_3 axis is much more difficult because among the eight triangle planes, two at the top and bottom surfaces possess smaller equilateral triangles, whereas the other six located in the side planes bear isosceles triangles. Therefore, to satisfy the geometrical requirement for trigonal antiprism, two different tritopic ligands should be used, including two C3-symmetry tripodal linkers and six single-arm lengthened tripodal linkers. Controlling the precise assembly of such a hybrid linker system to attain container structures with distinct geometric attributes has proven to be elusive.

Herein, we demonstrate an effective strategy involving replacing tripodal carboxylate linkers with those selectively elongated along one direction to desymmetrize an otherwise highly symmetric but nonreactive octahedral coordination container modulated its molecular recognition capability, and most significantly, switched on its supramolecular catalysis. Partially extending the regular C_3 -symmetry 1,3,5-benzenetricarboxylate (BTC) trigonal ligand by a benzylamino spacer provided the single-arm lengthened tricarboxylate ligand, 5-[(4-carboxybenzyl) amino]-isophthalic acid (L, Scheme 1b). Incorporation of the -CH2NH- unit in L not only improved the flexibility of the desymmetric tricarboxylate linkers, benefitting the assembly of desired irregular coordination containers but also introduced additional Brønsted basic active sites, potentially enhancing the catalytic activity of the nanocavity. The sulfonylcalix[4]arene-based tetranuclear cluster units35 (Scheme 1b) feature four convergent extends; thus, these vectors are a form of powerful building blocks for the fabrication of a new class of coordination containers. 31-33,36-38 Their remarkably robust architectures could tolerate the simple expansion of the endo cavity using elongated carboxylate linkers, and even allow more sophisticated desymmetrization of the cavity via the insertion of a secondary carboxylate linker with lower symmetry. As expected, a tetragonalelongated octahedral coordination container (1) was obtained using L as a single-arm lengthened tricarboxylate ligand (Scheme 1b). Furthermore, by judicious selection of cyclohexane-1,3,5-tricarboxylate (CTC) as a flexible C_3 -symmetry tricarboxylate linker to build two smaller equilateral triangles, as well as utilizing L as a single-arm lengthened tricarboxylate ligand to fabricate six isosceles triangles, trigonal-elongated octahedral (trigonal antiprismatic) coordination container (2) was successfully attained. We noted the importance of the desymmetrization here, as it became clear that the use of a partially elongated carboxylate linker could afford to expand the endo cavity symmetrically, and hence, modulate their molecular recognition capability and catalytic activity. Furthermore, the Knoevenagel condensation reaction was chosen as a model system to examine how the host-guest interactions and catalytic properties could be rationally engineered through precisely manipulated supramolecular hosts' structures.

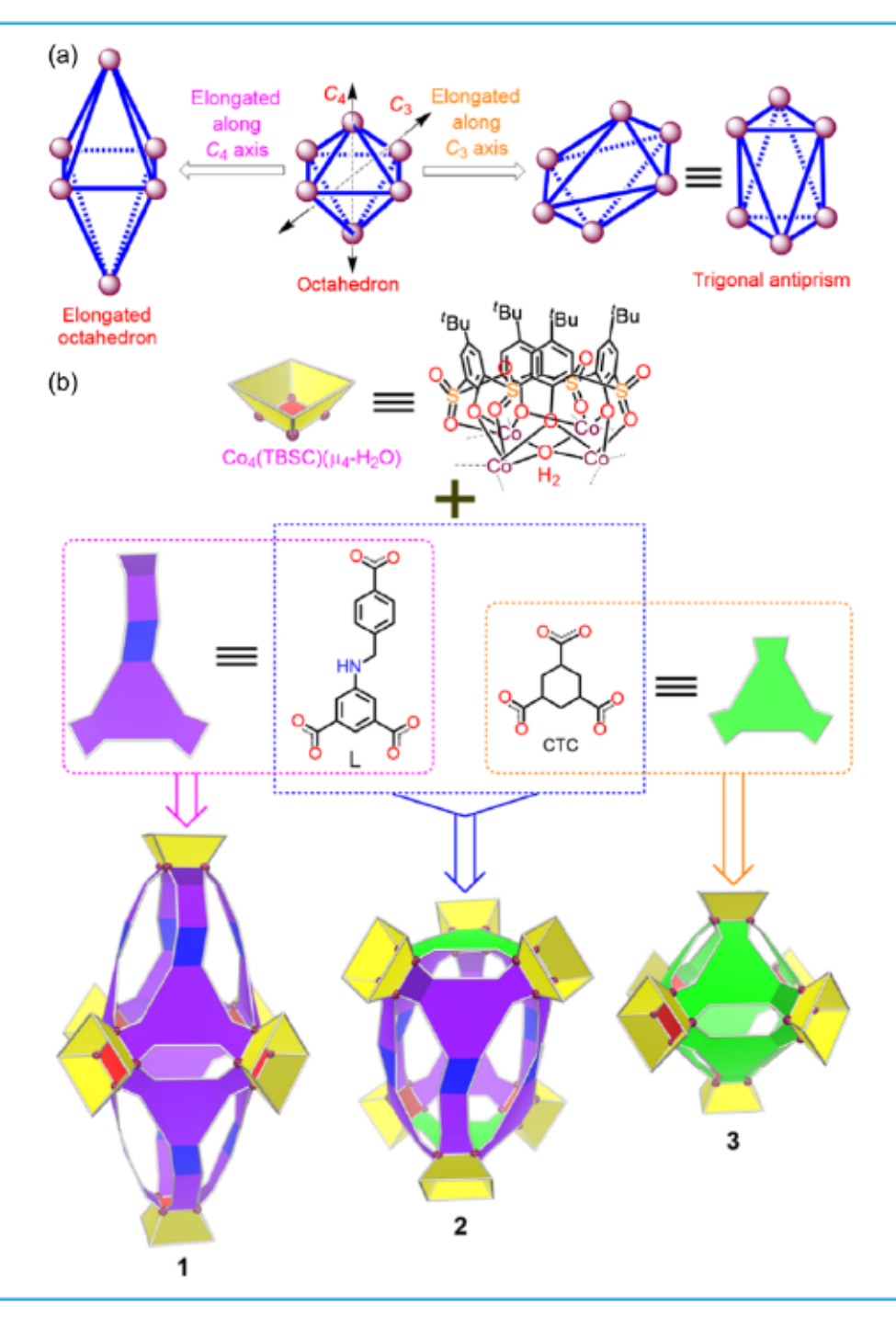
Experimental Methods

Synthesis of container 1

Hydrated cobalt chloride (CoCl₂•6H₂O; 59.50 mg, 0.25 mmol), H₃L (23.10 mg, 0.073 mmol), and *p-tert*-butylsulfonylcalix[4]arene (H₄TBSC; 42.15 mg, 0.05 mmol) were dissolved in dimethylformamide (DMF) (5 mL) in a scintillation vial (20-mL capacity), then 1 mL of methanol was added that produced a clear solution. The vial was

DOI: 10.31635/ccschem.021.202100987





Scheme 1 (a) Cartoon representation of the tetragonal (left), trigonal (right), and distortion of a regular octahedron (middle) elongating along the C_4 or C_3 rotation axis, respectively. (b) The design approach for the assembly of regular/distorted octahedral coordination containers based on symmetric and/or single-arm lengthened tricarboxylate linkers.

placed in a sand bath, then transferred to a programmable oven, and heated at a rate of 0.5 °C/min from 30 to 100 °C. The temperature was held at 100 °C for 24 h before the oven was cooled at a rate of 0.2 °C/min to 30 °C. Pink crystals of 1 were isolated by washing with DMF. The crystals were then vacuum dried at 100 °C to give rise to 41.59 mg of activated material. Yield: 54.9%. Fourier transform infrared (FT-IR) (KBr): $\nu = 2962$ (m), 1607 (vs),

1491 (vs), 1454 (s), 1416 (s), 1328 (s), 1263 (s), 1080 (m), 798 (m), 565 (vs) cm⁻¹.

Synthesis of container 2

 $CoCl_2$ •6 H_2O (59.50 mg, 0.25 mmol), H_3L (15.73 mg, 0.050 mmol), H_3CTC (3.60 mg, 0.0167 mmol), and H_4TBSC (42.15 mg, 0.05 mmol) were dissolved in DMF

DOI: 10.31635/ccschem.021.202100987



(5 mL) in a scintillation vial (20-mL capacity), then 3 mL of methanol was added that produced a clear solution. The vial was placed in a sand bath, then transferred to a programmable oven, and heated at a rate of 0.5 °C/min from 30 to 100 °C. The temperature was held at 100 °C for 24 h before the oven was cooled at a rate of 0.2 °C/min to 30 °C. Pink crystals of **2** were isolated by washing with acetone. Further solvent-exchange experiments were performed by soaking the crystals for 3 days in acetone, replenishing the acetone solvent three times. The crystals were then vacuum dried at 100 °C to give rise to 46.31 mg of activated material. Yield: 62.5%. FT-IR (KBr): ν = 2962 (m), 1607 (vs), 1491 (vs), 1454 (vs), 1415 (s), 1328 (m), 1263 (s), 1078 (m), 839 (m), 798 (s), 567 (vs) cm⁻¹.

Synthesis of container 3

CoCl₂•6H₂O (119.20 mg, 0.50 mmol), H₃CTC (32.41 mg, 0.15 mmol), and H₄TBSC (84.82 mg, 0.10 mmol) were dissolved in DMF (5 mL) in a scintillation vial (20-mL capacity), then 3 mL of methanol was added that produced a clear solution. The vial was placed in a sand bath, then transferred to a programmable oven, and heated at a rate of 0.5 °C/min from 30 to 100 °C. The temperature was held at 100 °C for 24 h before the oven was cooled at a rate of 0.2 °C/min to 30 °C. Pink crystals of 3 were isolated by washing with acetone. Further solvent-exchange experiments were performed by soaking the crystals in acetone for 3 days with the acetone solvent replenished three times. The crystals were then vacuum dried at 100 °C, giving rise to 73.30 mg of activated material. Yield: 53.0%. FT-IR (KBr): ν = 2962 (m), 1606 (vs), 1590 (s),1492 (vs), 1454 (s), 1419 (s), 1363 (m), 1331 (m), 1291 (m), 1263 (s), 1135(m), 1078 (s), 907 (m), 839 (m), 798 (s), 564 (vs) cm⁻¹.

Container catalyzed Knoevenagel condensation

Aromatic aldehyde (0.04 mmol), 1,3-indanedione (0.04 mmol), and coordination containers (8 mol%) were dissolved in chloroform (0.4 mL), which was stirred at 40 °C for 4-12 h. The organic fraction was collected by chromatography over a silica column using petroleum ether (PE):ethyl acetate (EA) = 5:1 (v:v) as the eluent. After solvent evaporation, the residue was redissolved in CDCl₃, and the conversion yield was determined by the proton nuclear magnetic resonance (1 H NMR) spectrum. Using the Me₃L as the catalyst, a control experiment was carried out under identical conditions, except 64 mol% of Me₃L and CDCl₃ were used.

Titration experiments

The solution host-guest chemistry was probed using the fluorescence titration technique. Stock solutions of the

guests were prepared in CHCl $_3$ at a concentration of ca. 3×10^{-5} M. Then 10.00 mL of the stock solution was used to dissolve an accurately known mass of container samples of 1, 2, or 3, chosen to yield a solution at a concentration 5–10 times higher than that of the guest. Subsequently, 2.00 mL of the guest solution was placed in a 10.0 mm quartz cell, upon which 5–200 μ L of the container solution was added gradually. After each addition, the cell was stoppered and inverted, collecting the fluorescence spectrum at 25 °C after 5 min to ensure complete mixing of the solution and reaching equilibration. To evaluate the overall binding strength, the titration results were fitted into the nonlinear Hill equation ^{39,40}:

$$\frac{\Delta I}{\Delta I_{\text{max}}} = \frac{K_{\text{a}}[H]_{\text{O}}^{n}}{1 + K_{\text{a}}[H]_{\text{O}}^{n}}$$

where $\Delta I (= I - I_0)$ is the change in emission intensity, $[H]_0$ is the initial containers' concentration, K_a is the association constant (dimensionless), and n is the Hill coefficient (dimensionless). A plot of ΔI against $[H]_0$ (in this study, $[H]_0 = [Host]$) was used to estimate ΔI_{max} , n, and K_a . The titration data are summarized in Supporting Information Tables S2–S7 and were fit to this model using the nonlinear regression method of the Origin 8.6 software (OriginLab Corp., Northampton, MA).

Results and Discussion

Synthesis and structure

Reaction of H₄TBSC and H₃L with cobalt(II) chloride in DMF/methanol mixture at 100 °C for 1 day gave rise to pink crystals of 1. As revealed by X-ray crystallography (Figure 1a and Supporting Information Table S1 and Figure S1), 1 adopted a structural topology of a highly tetragonal-elongated octahedron, strikingly contrasting to the regular octahedron derived from C_3 -symmetry BTC³² or that from CTC (3) as a result of single-arm elongation of tricarboxylate ligand L. To achieve trigonal distorted octahedron, BTC was first attempted to be used as a C_3 -symmetry tricarboxylate linker and \mathbf{L} as a single-arm lengthened tricarboxylate ligand. Unfortunately, only BTC-based MOSC-1-Co³² with regular octahedral geometry and tetragonal-elongated octahedral coordination container 1 could be isolated. This was likely due to the rigid planar structure of BTC, implying that the formation of the robust regular octahedral structure was more preferred. Subsequently, CTC with better flexibility was selected as a C₃-symmetry tricarboxylate linker in place of BTC to fabricate trigonal-elongated octahedral architecture. Indeed, a new phase of coordination container 2 was isolated successfully at a molar ratio of $TBSC: Co^{2}: H_3L: H_3CTC = 1:5:1:0.33$ under otherwise identical reaction conditions. The crystals' phase purity

DOI: 10.31635/ccschem.021.202100987



was unambiguously confirmed by consistent crystal morphology and single-crystal X-ray diffraction analysis conducted with randomly selected crystals from numerous reaction trials. In the case in which the ratio between H₃L and H₃CTC deviated from 1:0.33, the reactions gave rise to mixed products of 1 and 2 or 3, suggesting that container 2 was the thermodynamically stable product. Structural analysis revealed that 2 featured triangular antiprismatic architecture, also described as a trigonal-distorted octahedron was formed by the intense elongation along the C_3 rotation axis (Scheme 1). To the best of our knowledge, container 2 represented the first example of a coordination container originating from two different tripodal ligands, thereby signifying a new approach for the construction of multicomponent coordination containers.

As shown in Figure 1, whether irregular octahedral containers 1 and 2 or regular octahedral container 3 possesses six TBSC-based tetranuclear units, Co₄(TBSC)(μ₄-H₂O), that occupy the vertices of coordination container, thus, providing six exo cavities constructed by the upper rims of TBSC. The elongated octahedral coordination container 1 (Figure 1a) consists of six $Co_4(TBSC)(\mu_4-H_2O)$ units linked by eight single-arm lengthened tricarboxylate ligands L residing on the eight triangle faces to generate a prolate spheroid-shaped endo cavity with the equatorial and longitudinal dimensions of ca. 11 x 27 Å. Container 2 (Figure 1b and Supporting Information Figure S2) with trigonal antiprismatic architecture is made up of six Co₄(TBSC)(μ₄-H₂O) units, six single-arm lengthened tricarboxylate linkers (L) located at six triangular side faces, and two C3-symmetry CTC connectors situated on two basal faces to give a cylinder-shaped cavity with radius and height of ca. 9 and 15 Å, respectively. In contrast, container 3 (Figure 1c and Supporting Information Figure S3) with a regular octahedral architecture displayed a spherical endo cavity with a diameter of ca. 12.5 Å. Notably, even though the shapes of the endo cavities in containers 1 and 2 were distinctly different, they consisted of comparable internal volumes of ca. 1 nm3 (Supporting Information Figures S4 and S5), which were almost twice as that of 3 (ca. 0.6 nm³; Supporting Information Figure S6). Container 1 has two types of windows, including four small openings with dimensions of ca. 1.0×2.3 Å, similar to those observed in BTC-based MOSC-1-Co32 and eight much longer window apertures with a length of ca. 8.6 Å accompanying the smallest and longest width of 1.2 and 2.6 Å, respectively. Container 2 also possessed two types of openings, containing six small windows (ca. $1.0 \times 2.3 \text{ Å}$) and six elongated portals (ca. $8.6 \times 1.7 \text{ Å}$). In contrast, container 3 only had 12 small portals with dimensions of ca. 1.0 x 2.3 Å. Undoubtedly, the varied shapes, sizes, and windows of endo cavities in coordination containers 1-3 provide feasibility to regulate encapsulation capacity for guests with specific geometric characteristics.

(a) (c)

Figure 1 | Perspective views of coordination container 1 (a), 2 (b), and 3 (c) from X-ray crystallography. The well-defined endo cavities are shown in yellow spheroid.

Host-guest chemistry

To demonstrate how the structures of coordination containers can be precisely manipulated to engineer the catalytic reactivity rationally, the Knoevenagel condensation reaction was chosen as a model system to examine the catalytic activity of predesigned coordination containers 1–3. The host-guest chemistry of 1–3 was initially analyzed using the aldehyde substrates (Scheme 2) of 2-anthraldehyde (4i) and 1-pyrenecarboxaldehyde (4j) as representative guests through the fluorescence spectroscopic titration experiments. Upon the gradual addition of container 1 to 4i solution in CHCl₃, the fluorescence spectrum of 4i

DOI: 10.31635/ccschem.021.202100987



Scheme 2 | (a) Reaction scheme of Knoevenagel condensation of 1,3-indanedione and aromatic aldehydes. (b) Structures of arylaldehyde substrates used in this study.

centered at 470 nm decreases gradually (Supporting Information Figure S7), indicating the formation of host-guest complexes through encapsulation of 4i into the *endo* cavity of container 1. The fitting of the titration

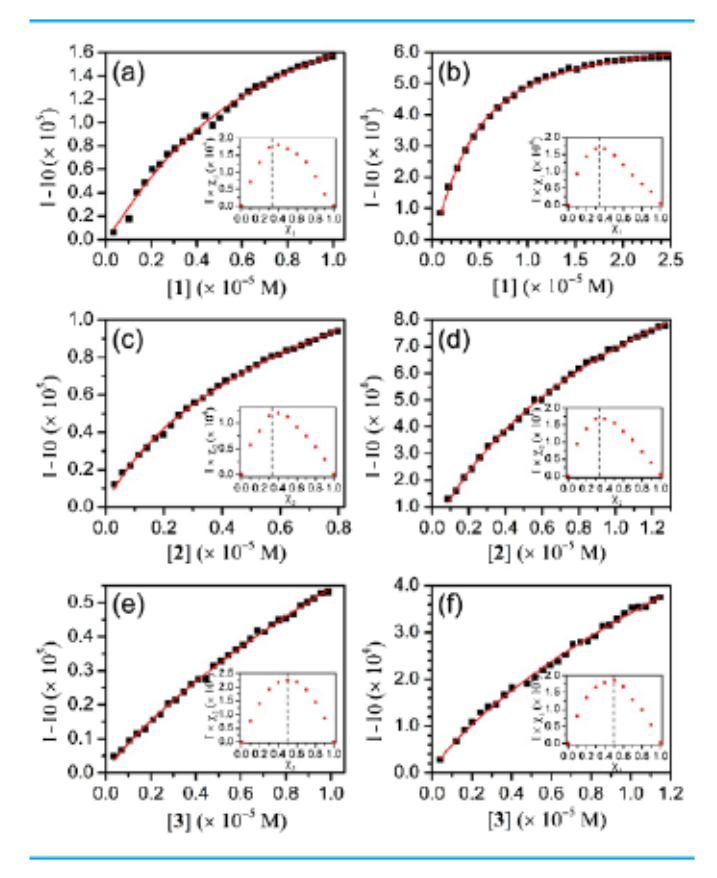


Figure 2 | Nonlinear curve fitting to Hill equation using data from fluorescence titration of 2-anthraldehyde (4i) with 1 (a), 2 (c), and 3 (e), and 1-pyrenecarboxaldehyde (4j) with 1 (b), 2 (d), and 3 (f). The insets show the Job's plots.

Table 1 | Association Constant (K_a) and Binding Stoichiometry of Containers **1-3** Determined by the Titration Experiments and Job's Method, Respectively

Host	Guest	$K_{\rm a}$	Host:Guest	
1	4i	$(16.4 \pm 2.5) \times 10^4$	1:2	
2	4i	$(8.83 \pm 1.82) \times 10^4$	1:2	
3	4i	$(1.19 \pm 0.92) \times 10^4$	1:1	
1	4j	$(23.5 \pm 0.4) \times 10^4$	1:2	
2	4j	$(6.33 \pm 0.93) \times 10^4$	1:2	
3	4 j	$(1.28 \pm 0.05) \times 10^4$	1:1	

data with the Hill equation gave rise to the association constant of 1.64×10^5 . The host-guest stoichiometry of 1 and 4i was further estimated to be ca. 2:1 based on the Job's plot approach (Figure 2a, inset). Similar host-guest interactions were also observed when containers 2 and 3 were used as host molecules (Figures 2c and 2e and Supporting Information Figures S8 and S9). When similar titration experiments were performed on containers 2 and 3, the binding affinity between 2 and 4i was determined to be 8.83 x 104, lower than that of 1 but remarkably higher than that of 3 (1.19 \times 10⁴) (Table 1). Based on Job's plots (Figures 2c and 2e, insets), the binding stoichiometry of 2 was calculated to be ca. 2:1, while container 3 exhibited only one equivalent of uptake. Moreover, guest 1-pyrenecarboxaldehyde (4j) (Figures 2b, 2d, and 2f and Supporting Information Figures S10-S12) behaved quite similar to guest 4i with the larger binding constant of 2.35 × 10⁵ between 1 and 4j. The binding affinities displayed the order of 1 > 2 > 3, which indicated the extended π -conjugated system in single-arm lengthened tricarboxylate linker L could benefit to strengthen the host-guest binding affinity. Therefore, modifying the character of tricarboxylate ligands provided a feasible approach to regulate host-guest binding properties of coordination containers by topological modulation. The higher binding capacity of container 1 or 2 was ascribed to the elongated endo cavity in 1 or 2 that is feasible for loading two guest molecules oriented presumably in a close π - π stacking pattern, thereby increasing the local concentration of reaction substrates and promoting the catalytic conversion yield.

Catalytic reactivity

Based on the host-guest properties between coordination containers 1-3 and arylaldehyde substrates, we next examined the catalytic activity of coordination containers 1-3 to Knoevenagel condensation reaction, which is typically catalyzed by Lewis/Brønsted-base⁴¹⁻⁴⁵ and also realizable through Lewis-acid catalysts in some cases.⁴⁶⁻⁴⁸ The catalytic reactions were carried out in the presence of 1-3 using 1,3-indanedione and various

DOI: 10.31635/ccschem.021.202100987



Table 2 | Yields for Knoevenagel Condensation Reactions of 1,3-Indanedione and Aromatic Aldehydes Catalyzed by Containers 1-3 or Ligand Trimethyl Ester (Me₃L) in CHCl₃ Solution at 40 °C

		Reaction		Yield (%) ^a			
Entry	Substrate	Time (h)	16	2 ^b	3 ^b	Me ₃ L ^c	Blank
1	4a	5	99	93	4	18	<1
2	4b	4	99	99	44	26	<1
3	4c	6	99	92	1	11	<1
4	4d	6	90	87	1	6	<1
5	4e	6	96	95	65	1	<1
6	4f	6	91	87	81	6	<1
7	4g	6	99	88	76	12	<1
8	4h	12	91	93	4	35	<1
9	4i	12	78	62	1	21	<1
10	4j	12	89	53	5	8	<1
11	4k	12	12	7	<1	<1	<1

- ^a Estimated by ¹H NMR spectra.
- ^b 8 mol % of 1, 2, or 3 was used.
- 64 mol % of Me3L was used.

aromatic aldehydes (4a-4k) as reaction substrates (Schemes 2a and 2b). Contrast experiments were also performed without the addition of a catalyst or using trimethyl ester of H_3L (Me_3L) in place of 1-3 as a catalyst. The conversion yields were estimated from 1H NMR spectra. The stability of catalysis 1-3 was further confirmed through the UV-vis spectrometry studies of containers 1-3 before and after catalytic reactions (Supporting Information Figures S13-S15).

As listed in Table 2, the condensation reaction between arylaldehyde and 1,3-indanedione does not occur in the absence of a catalyst. The Me₃L bearing the Brønstedbasic -CH₂NH- site showed some degree of catalytic activity, attributed to the catalytic activity of -CH2NHbasic center. For regular octahedral container 3, certain catalytic activity was only observed when benzaldehyde derivatives (Table 2, entries 2 and 5-7) were used as a substrate. The catalytic reactivity of 3 was likely promoted by Brønsted-acid centers of µ4-H2O in the internal cavities of TBSC-based octahedral containers.⁴⁹ Therefore, the small endo cavity of container 3 only allowed the more minor and highly reactive substrate to approach the µ4-H2O active sites and subsequently activated the aldehyde substrates for Knoevenagel condensation.

Remarkably, the supramolecular catalytic activity is distinctly activated when the elongated octahedral coordination containers 1 or 2 were used as a catalyst. Containers 1 and 2 featuring larger internal cavities displayed much higher conversion yields than those of 3 and Me₃L (Table 2). Particularly, container 1 gave a significantly higher conversion yield than those of 2 and 3 to the catalytic condensation of the bulkier substrate of

1-pyrenecarboxaldehyde (4j) (89% for 1 vs 53% for 2 and 5% for 3), possibly because of the longer internal cavity in 1 is more suitable for effectively encapsulating reaction substrates than the cramped cylinder-shaped *endo* cavity in 2. As a result, the shape and size of the *endo* cavity in the coordination container behaved as regulators to manipulate the catalytic reactivity.

Catalytic mechanism

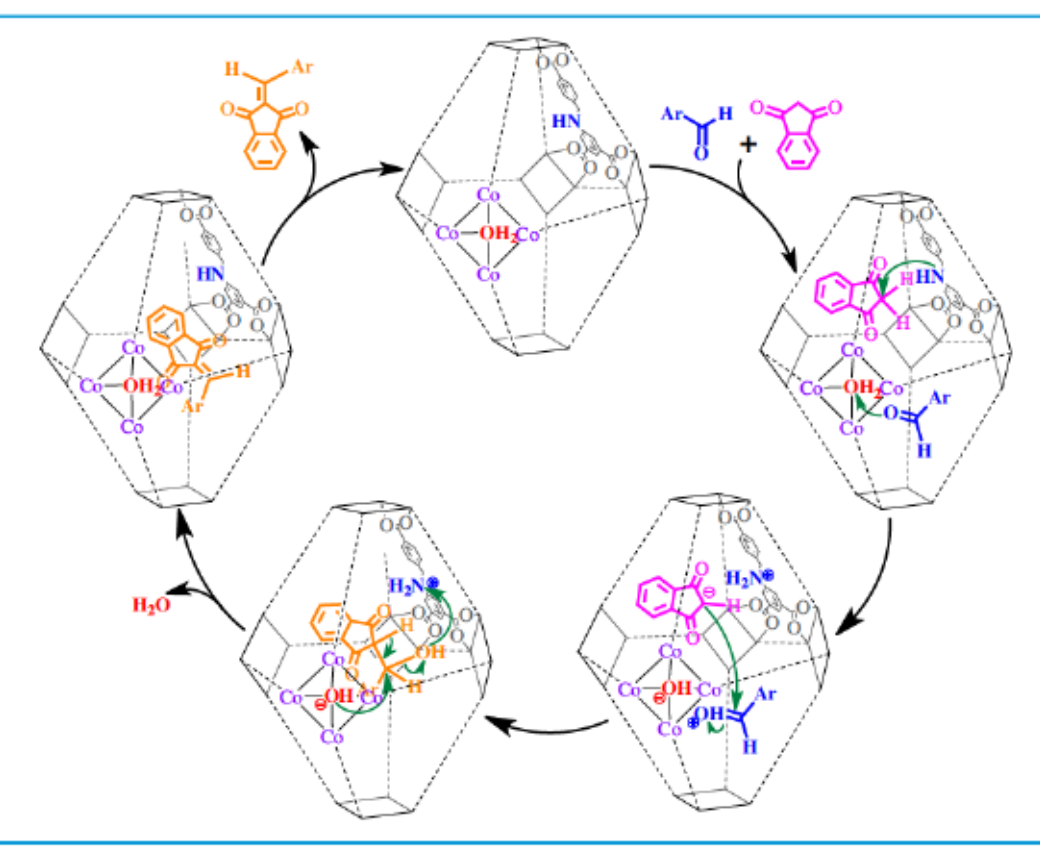
The elongated containers 1 and 2 possessed a much larger endo cavity and additional Brønsted-basic (-CH₂NH-) functional groups. Thus, the catalytic activity of container 1 or 2 was most likely derived from the catalytic cooperative effect of Brønsted acid-base dual active centers of Brønsted acid (µ4-H2O) and base (-CH₂NH-) sites. The supramolecular catalytic activities of these synthetic containers were highly dependent on the geometry of internal cavities, suggesting the Brønsted acid (μ₄-H₂O) sites catalytic mechanism.⁴⁹ Extending the internal cavities of synthetic containers benefitted an efficient activation of the aldehyde units by the Brønsted acidic (µ4-H2O) centers, hence, boosted the conversion yield. This could be proved further when 9-anthraldehyde (4k) with aldehyde group bound to a dumpy polycyclic aromatic body was employed as a substrate, which processed a relatively lower conversion yield when 1 or 2 was used as a catalyst (Table 2, entry 11) due to the steric constraint of the dumpy polycyclic aromatic body that most likely prohibited the aldehyde groups from approaching proximity of the Brønsted acidic μ₄-H₂O catalytic centers in the endo cavity.

The -CH₂NH- functionalized tricarboxylate ligands (**L**) built-in containers **1** and **2** also play a key role in the catalytic process. On the one hand, the -CH₂NH- units can serve as Brønsted base active center to enhance the catalytic reactivity. ^{49,50} The overall best catalysis of container **1** could also be attributed to the incorporation of more -CH₂NH- functionalized bridging ligands (eight **L**) and thus, more Brønsted base (-CH₂NH-) catalytic sites than those of **2** (six **L** ligands) and **3** (without **L** ligands). On the other hand, ligand **L** in containers **1** and **2** adopted a nearly planar configuration, appropriate for close contact with 1,3-indanedione through π - π interactions, allowing the -CH₂NHPh- reactive site to approach the activated methylene center.

Based on the above discussion, a plausible acid-base dual catalytic mechanism for the Knoevenagel condensation catalyzed by containers 1 and 2 was proposed, as indicated in Scheme 3, as follows: Once the substrates (arylaldehyde and activated methylene derivatives) are encapsulated into the *endo* cavity of coordination container, the activated methylene is deprotonated by -NH- Brønsted-base center to give carbanion. Meanwhile, the Brønsted-acid center of Co_4 -bound μ_4 - H_2O synchronously protonates the carbonyl group of

DOI: 10.31635/ccschem.021.202100987





Scheme 3 | Proposed mechanism for the Knoevenagel condensation catalyzed by containers 1 and 2.

arylaldehyde. Subsequently, the carbanion immediately attacks the protonated arylaldehydes to form a β -hydroxy intermediate, followed by rearrangement and dehydration of the intermediate to regenerate the catalyst and yield the final olefin product.

Conclusion

We have demonstrated a feasible synthetic approach to achieve elaborately designed tetragonal- and trigonalelongated octahedral coordination containers along C4 and C3 symmetric axes using single-arm lengthened tricarboxylate ligands to associate with sulfonylcalixarenecapped tetranuclear clusters. The judicious selection of flexible C3-symmetry CTC and methylene aminofunctionalized single-arm lengthened tricarboxylate ligands resulted in the isolation and crystallographic characterization of an unprecedented distorted octahedral coordination container, that is, a trigonal antiprismatic architecture based on Co4 cluster units. Both the host-guest interaction and catalytic activity could be manipulated judiciously through topological modulation of internal cavities in coordination containers using functionalized single-arm lengthened tricarboxylate ligand. The combination of both Brønsted-acidic (µ4-H2O) and Brønsted-basic (-NH-) centers allowed the attainment of the acid-base dual catalytic reactivity toward the Knoevenagel condensation. Thus, this geometrical manipulation

strategy provides a new approach for conveniently designing multifunctional metal-organic materials.

Supporting Information

Supporting Information is available and includes additional experimental details, synthesis procedures of ligands, additional figures (PDF), and crystallographic information (CIF).

Conflict of Interest

There is no conflict of interest to report.

Funding Information

This work was supported by the National Natural Science Foundation of China (grant nos. 21673239, 21501179, and 21531008), Natural Science Foundation of Fujian Province (grant no. 2017J06008), the CAS/SAFEA International Partnership Program for Creative Research Teams, and the Strategic Priority Research Program of the Chinese Academy of Sciences (grant no. XDB20000000). Z.W. acknowledges a National Science Foundation CAREER award (grant no. CHE-1352279) for supporting work related to the design and synthesis of container molecules, a second NSF grant (grant no. CHE-1800354) for supporting work pertaining to

DOI: 10.31635/ccschem.021.202100987



supramolecular catalysis, and the South Dakota Governor's Office of Economic Development through the Center for Fluorinated Functional Materials for additional financial support.

References

- Lehn, J. M. Supramolecular Chemistry; VCH Publishing: Weinheim, Germany, 1995.
- Fyfe, M. C. T.; Stoddart, J. F. Synthetic Supramolecular Chemistry. Acc. Chem. Res. 1997, 30, 393-401.
- Lehn, J.-M. Supramolecular Chemistry—Scope and Perspectives Molecules, Supermolecules, and Molecular Devices (Nobel Lecture). Angew. Chem. Int. Ed. Engl. 1988, 27, 89-112.
- Pignataro, B. Molecules at Work: Selfassembly, Nanomaterials, Molecular Machinery; Wiley-VCH: Weinheim, Germany, 2012.
- Cook, T. R.; Zheng, Y. R.; Stang, P. J. Metal-Organic Frameworks and Self-Assembled Supramolecular Coordination Complexes: Comparing and Contrasting the Design, Synthesis, and Functionality of Metal-Organic Materials. Chem. Rev. 2013, 113, 734-777.
- Li, X.-X.; Zhao, D.; Zheng, S.-T. Recent Advances in POM-Organic Frameworks and POM-Organic Polyhedra. Coord. Chem. Rev. 2019, 397, 220-240.
- Chang, X.; Zhou, Z.; Shang, C.; Wang, G.; Wang, Z.; Qi, Y.;
 Li, Z. Y.; Wang, H.; Cao, L.; Li, X.; Fang, Y.; Stang, P. J.
 Coordination-Driven Self-Assembled Metallacycles Incorporating Pyrene: Fluorescence Mutability, Tunability, and Aromatic Amine Sensing. J. Am. Chem. Soc. 2019, 141, 1757–1765.
- 8. Tang, J.-H.; Sun, Y.; Gong, Z.-L.; Li, Z.-Y.; Zhou, Z.; Wang, H.; Li, X.; Saha, M. L.; Zhong, Y.-W.; Stang, P. J. Temperature-Responsive Fluorescent Organoplatinum(II) Metallacycles. J. Am. Chem. Soc. 2018, 140, 7723-7729.
- 9. Zhang, M.; Saha, M. L.; Wang, M.; Zhou, Z.; Song, B.; Lu, C.; Yan, X.; Li, X.; Huang, F.; Yin, S.; Stang, P. J. Multicomponent Platinum(II) Cages with Tunable Emission and Amino Acid Sensing. *J. Am. Chem. Soc.* **2017**, *139*, 5067-5074.
- Mendez-Arroyo, J.; Barroso-Flores, J.; Lifschitz, A. M.;
 Sarjeant, A. A.; Stern, C. L.; Mirkin, C. A. A Multi-State,
 Allosterically-Regulated Molecular Receptor with Switchable Selectivity. J. Am. Chem. Soc. 2014, 136, 10340-10348.
- Rizzuto, F. J.; Carpenter, J. P.; Nitschke, J. R. Multisite Binding of Drugs and Natural Products in an Entropically Favorable, Heteroleptic Receptor. J. Am. Chem. Soc. 2019, 141, 9087-9095.
- Lehn, J. M. Toward Self-Organization and Complex Matter. Science 2002, 295, 2400-2403.
- Ariga, K.; Ito, H.; Hill, J. P.; Tsukube, H. Molecular Recognition: From Solution Science to Nano/Materials Technology. Chem. Soc. Rev. 2012, 41, 5800-5835.
- Mahon, C. S.; Fulton, D. A. Mimicking Nature with Synthetic Macromolecules Capable of Recognition. *Nat. Chem.* 2014, 6, 665–672.
- Takezawa, H.; Akiba, S.; Murase, T.; Fujita, M. Cavity-Directed Chromism of Phthalein Dyes. J. Am. Chem. Soc. 2015, 137, 7043-7046.

- Sawada, T.; Hisada, H.; Fujita, M. Mutual Induced Fit in a Synthetic Host-Guest System. J. Am. Chem. Soc. 2014, 136, 4449-4451.
- 17. Ronson, T. K.; Meng, W.; Nitschke, J. R. Design Principles for the Optimization of Guest Binding in Aromatic-Paneled Fe^{II}₄L₆ Cages. *J. Am. Chem. Soc.* **2017**, *139*, 9698-9707.
- Zhao, C.; Toste, F. D.; Raymond, K. N.; Bergman, R. G. Nucleophilic Substitution Catalyzed by a Supramolecular Cavity Proceeds with Retention of Absolute Stereochemistry. J. Am. Chem. Soc. 2014, 136, 14409-14412.
- Tan, C.; Jiao, J.; Li, Z.; Liu, Y.; Han, X.; Cui, Y. Design and Assembly of a Chiral Metallosalen-Based Octahedral Coordination Cage for Supramolecular Asymmetric Catalysis. Angew. Chem. Int. Ed. 2018, 57, 2085–2090.
- Mouarrawis, V.; Plessius, R.; van der Vlugt, J. I.; Reek, J. N.
 H. Confinement Effects in Catalysis Using Well-Defined Materials and Cages. Front. Chem. 2018, 6, 623.
- Cullen, W.; Takezawa, H.; Fujita, M. Demethylenation of Cyclopropanes via Photoinduced Guest-to-Host Electron Transfer in an M6 L4 Cage. *Angew. Chem. Int. Ed.* 2019, 58, 9171-9173.
- Tan, C.; Chu, D.; Tang, X.; Liu, Y.; Xuan, W.; Cui, Y. Supramolecular Coordination Cages for Asymmetric Catalysis. Chem. Eur. J. 2019, 25, 662-672.
- Ueda, Y.; Ito, H.; Fujita, D.; Fujita, M. Permeable Self-Assembled Molecular Containers for Catalyst Isolation Enabling Two-Step Cascade Reactions. J. Am. Chem. Soc. 2017, 139, 6090-6093.
- Nitschke, J. R. Construction, Substitution, and Sorting of Metallo-Organic Structures via Subcomponent Self-Assembly. Acc. Chem. Res. 2007, 40, 103-112.
- Chakrabarty, R.; Mukherjee, P. S.; Stang, P. J. Supramolecular Coordination: Self-Assembly of Finite Two- and Three-Dimensional Ensembles. Chem. Rev. 2011, 111, 6810-6918.
- Datta, S.; Saha, M. L.; Stang, P. J. Hierarchical Assemblies of Supramolecular Coordination Complexes. Acc. Chem. Res. 2018, 51, 2047–2063.
- Debata, N. B.; Tripathy, D.; Sahoo, H. S. Development of Coordination Driven Self-Assembled Discrete Spherical Ensembles. Coord. Chem. Rev. 2019, 387, 273-298.
- 28. Plajer, A. J.; Percastegui, E. G.; Santella, M.; Rizzuto, F. J.; Gan, Q.; Laursen, B. W.; Nitschke, J. R. Fluorometric Recognition of Nucleotides within a Water-Soluble Tetrahedral Capsule. *Angew. Chem. Int. Ed.* **2019**, *58*, 4200-4204.
- 29. Jimenez, A.; Bilbeisi, R. A.; Ronson, T. K.; Zarra, S.; Woodhead, C.; Nitschke, J. R. Selective Encapsulation and Sequential Release of Guests within a Self-Sorting Mixture of Three Tetrahedral Cages. *Angew. Chem. Int. Ed.* **2014**, *53*, 4556–4560.
- Yan, K.; Dubey, R.; Arai, T.; Inokuma, Y.; Fujita, M. Chiral Crystalline Sponges for the Absolute Structure Determination of Chiral Guests. J. Am. Chem. Soc. 2017, 139, 11341–11344.
- 31. Liu, M.; Liao, W. P.; Hu, C. H.; Du, S. C.; Zhang, H. J. Calixarene-Based Nanoscale Coordination Cages. *Angew. Chem. Int. Ed.* **2012**, *51*, 1585-1588.

DOI: 10.31635/ccschem.021.202100987



- Dai, F.-R.; Wang, Z. Modular Assembly of Metal-Organic Supercontainers Incorporating Sulfonylcalixarenes. J. Am. Chem. Soc. 2012, 134, 8002–8005.
- Hang, X.; Liu, B.; Zhu, X.; Wang, S.; Han, H.; Liao, W.; Liu,
 Y.; Hu, C. Discrete {Ni₄₀} Coordination Cage: A
 Calixarene-Based Johnson-Type (J₁₇) Hexadecahedron. J.
 Am. Chem. Soc. 2016, 138, 2969-2972.
- 34. Geng, D.; Han, X.; Bi, Y.; Qin, Y.; Li, Q.; Huang, L.; Zhou, K.; Song, L.; Zheng, Z. Merohedral Icosahedral M₄₈ (M = Co^{II}, Ni^{II}) Cage Clusters Supported by Thiacalix[4]arene. *Chem. Sci.* **2018**, *9*, 8535–8541.
- 35. Kajiwara, T.; Kobashi, T.; Shinagawa, R.; Ito, T.; Takaishi, S.; Yamashita, M.; Iki, N. Highly Symmetrical Tetranuclear Cluster Complexes Supported by *p-tert*-Butylsulfonylcalix [4]arene as a Cluster-Forming Ligand. *Eur. J. Inorg. Chem.* **2006**, *2006*, 1765–1770.
- 36. Xiong, K.; Jiang, F.; Gai, Y.; Yuan, D.; Chen, L.; Wu, M.; Su, K.; Hong, M. Truncated Octahedral Coordination Cage Incorporating Six Tetranuclear-Metal Building Blocks and Twelve Linear Edges. *Chem. Sci.* **2012**, *3*, 2321–2325.
- Bi, Y.; Du, S.; Liao, W. Thiacalixarene-Based Nanoscale Polyhedral Coordination Cages. Coord. Chem. Rev. 2014, 276, 61-72.
- Wang, S.; Gao, X.; Hang, X.; Zhu, X.; Han, H.; Li, X.; Liao, W.; Chen, W. Calixarene-Based (Ni₁₈) Coordination Wheel: Highly Efficient Electrocatalyst for the Glucose Oxidation and Template for the Homogenous Cluster Fabrication. J. Am. Chem. Soc. 2018, 140, 6271-6277.
- 39. Weiss, J. N. The Hill Equation Revisited: Uses and Misuses. FASEB J. 1997, 11, 835-841.
- Hill, A. V. The Possible Effects of the Aggregation of the Molecules of Hæmoglobin on Its Dissociation Curves. J. Physiol. 1910, 40, iv-vii.

- Knoevenagel, E. Condensation von Malonsäure mit Aromatischen Aldehyden Durch Ammoniak und Amine. Ber. Dtsch. Chem. Ges. 1898, 31, 2596–2619.
- 42. Ebitani, K.; Motokura, K.; Mori, K.; Mizugaki, T.; Kaneda, K. Reconstructed Hydrotalcite as a Highly Active Heterogeneous Base Catalyst for Carbon-Carbon Bond Formations in the Presence of Water. J. Org. Chem. 2006, 71, 5440-5447.
- Fioravanti, S.; Pellacani, L.; Tardella, P. A.; Vergari, M. C. Facile and Highly Stereoselective One-Pot Synthesis of Either (E)- or (Z)-Nitro Alkenes. *Org. Lett.* 2008, 10, 1449–1451.
- Lee, A.; Michrowska, A.; Sulzer-Mosse, S.; List, B. The Catalytic Asymmetric Knoevenagel Condensation. *Angew. Chem. Int. Ed.* 2011, 50, 1707–1710.
- List, B. Emil Knoevenagel and the Roots of Aminocatalysis. Angew. Chem. Int. Ed. 2010, 49, 1730-1734.
- Scott, J. L.; Raston, C. L. Solvent-Free Synthesis of 3-Carboxycoumarins. Green Chem. 2000, 2, 245–247.
- 47. Loh, T.-P.; Wei, L.-L. Indium-Trichloride Catalyzed Michael Reaction of Silyl Enol Ethers with α , β -Unsaturated Carbonyl Compounds Under Neat Condition. *Tetrahedron* **1998**, *54*, 7615–7624.
- Shanthan Rao, P.; Venkataratnam, R. V. Zinc Chloride as a New Catalyst for Knoevenagel Condensation. *Tetrahedron Lett.* 1991, 32, 5821–5822.
- Qiao, Y.; Zhang, L.; Li, J.; Lin, W.; Wang, Z. Switching on Supramolecular Catalysis via Cavity Mediation and Electrostatic Regulation. *Angew. Chem. Int. Ed.* 2016, 55, 12778–12782.
- Dai, F.-R.; Qiao, Y.; Wang, Z. Designing Structurally Tunable and Functionally Versatile Synthetic Supercontainers. *Inorg. Chem. Front.* 2016, 3, 243–249.

DOI: 10.31635/ccschem.021.202100987